# Transient structures in the twist Fréedericksz transition of low-molecular-weight nematic liquid crystals

M. Grigutsch, N. Klöpper, H. Schmiedel, and R. Stannarius
*Fachbereich Physik der Universität Leipzig, Linnéstrasse 5, D-04103 Leipzig, Federal Republic of Germany*
(Received 7 June 1993)

We have investigated the evolution of transient structures in the twist Fréedericksz transition of low-molecular-weight nematic liquid crystals. Planarly aligned cells have been exposed to an in-plane external magnetic field perpendicular to the initial director orientation. The formation of periodic structures was studied by conventional microscopy. We observed a complex director deformation showing an induced out-of-plane tilt. We describe the formation of periodic long-term stable twist-bend inversion walls which can be observed up to several hours after their appearance. The wavelengths of the structures determined experimentally are discussed and compared to theoretical predictions.

PACS number(s): 61.30.Gd, 47.20.−k, 61.30.Eb

## I. INTRODUCTION

In nature, processes far from equilibrium are often connected with the formation of transient periodic structures, developing from a homogeneous state by spontaneous local symmetry breaking [1]. It was discovered already a decade ago [2] that the reorientation of liquid crystals (LC) in destabilizing external fields such as, e.g., electric or magnetic fields, belongs to this class of processes. Liquid crystals may serve as simple and experimentally straightforward models for spontaneous structure formation.

There is broad experimental evidence of the formation of transient spatial structures in the Fréedericksz transition of nematic liquid crystals. In the most simple cases, the patterns consist of equidistant parallel stripes perpendicular to the initial director [2–6]. Oblique and two-dimensional structures [7,4,8] have also been observed. The structures are formed by periodic domains the directors of which reorient in opposite but equivalent directions. The periodically modulated director field is coupled dynamically to a mass flux which reinforces the inhomogeneous director reorientation due to the anisotropic viscosity of the nematic state. The characteristic periodicity of the pattern is usually described in terms of a most instable mode which dominates all slower modes during the decay of the initial instable equilibrium state. This mode is finally observed macroscopically. Its wavelength can be found by means of a linear stability analysis [9] of the governing nematodynamic equations [10]. Though the calculated dependence of this wavelength on the external field strength has been found to be in good agreement with experimental observations by several authors [2,3], significant deviations from the theoretical predictions have been reported by others [6].

The formation of transient patterns in lyotropic [7,3,4,6,11,12] and polymer LC systems [5,8,13] has been investigated by many groups. There are, however, only few data concerning such effects in ordinary low-molecular-mass thermotropic nematics [2,3,9]. In these systems, the time scale of the director reorientation is faster by orders of magnitude. Therefore, transient dissipative structures have gained attractiveness for experimentalists only after the development of modern video equipment [14].

We have studied the dynamics of transient structures in the magnetic-field-induced twist Fréedericksz transition in planar cells with low-molecular-weight nematic liquid crystals. The evolution of these structures has been recorded by means of a video camera mounted on a microscope. Unexpectedly, we observed the formation of complex structures which are long-term stable. These patterns are formed by periodic metastable twist-bend inversion walls, very similar to those reported for lyotropic systems [4,3]. They have not been observed previously in the twist Fréedericksz transition of low-molecular-weight nematics. We measured the periodicity of the walls in dependence on the external magnetic field strength and compared the results to predictions of the linearized mode selection theory. Furthermore, we have calculated the director field within the inversion walls numerically by free energy minimization.

This paper is organized as follows. In Sec. II a brief summary of the linear theory of mode selection in the twist Fréedericksz transition is given. The experimental setup is described in Sec. III. In Sec. IV we present the results of our experiments and numerical calculations. Section V summarizes the conclusions.

## II. LINEARIZED MODE SELECTION THEORY

We consider a nematic layer of thickness $d$ that is confined between two glass plates which provide uniform rigid planar anchoring of the nematic director. Suppose that at time $t=0$ an external magnetic field is switched on in the plane of the layer but perpendicular to the uniform initial director orientation. For positive diamagnetic susceptibility anisotropy $\Delta\chi$, the magnetic free energy is

 

minimum for a director alignment parallel to the external magnetic field. A uniform director reorientation is hindered, however, by the boundaries. At external fields exceeding a certain threshold, the so-called Fréedericksz field, a static elastic director deformation will arise which is homogeneous in the plane of the cell but inhomogeneous along the direction normal to the layer. This new stationary state will be reached in the time limit $t = \infty$. At intermediate times $0 < t < \infty$, dissipative structures may arise. Although they are unstable with respect to free energy considerations, periodic structures are preferred from a dynamic point of view because they show a considerably reduced effective viscosity due to backflow coupling. Thus their response to external field changes is faster compared to the homogeneous Fréedericksz transition.

When the external field is switched on, the sample is in an unstable equilibrium and small (thermal) fluctuations of the director field grow exponentially under the influence of the destabilizing external field. Because of inherent nonlinearities, the mode with the fastest growth rate suppresses all slower modes and is finally observed macroscopically.

The theoretical description of the mode selection was developed by Guyon, Meyer, and Salan [9] and it was applied to the twist geometry, e.g., by Fraden and coworkers [2,3]. They performed a linear stability analysis of the hydrodynamic equations. Since the periodic stripes found in the twist transition in a variety of systems are always perpendicular to the undisturbed director $\vec{n}_0$, homogeneity in the direction normal to $\vec{n}_0$ is assumed. With this assumption, the fastest growing mode is a planar one, the director of which is periodically modulated in the plane of external field and initial director orientation. The governing hydrodynamic equations for small amplitudes of the director distortion are given by the linearized torque balance (1) and the linearized Navier-Stokes equation (2), where inertia terms have been neglected,

$$\gamma_1 \dot{n}_y = -\alpha_2 \partial_x v_y + K_2 \partial_z^2 n_y + K_3 \partial_x^2 n_y + \frac{\Delta\chi}{\mu_0} B^2 n_y \ , \quad (1)$$

$$0 = \alpha_2 \partial_x (\dot{n}_y) + \eta_c \partial_x^2 v_y + \eta_a \partial_z^2 v_y \ , \quad (2)$$

$$\partial_\alpha \equiv \frac{\partial}{\partial \alpha} \ (\alpha = x, z), \quad \dot{n}_y \equiv dn_y/dt \ .$$

A Cartesian coordinate system has been introduced according to Fig. 1, where the $z$ axis corresponds to the layer normal, the $y$ axis is along the magnetic field, and the $x$ axis is along the undisturbed director $\vec{n}_0$. The periodically modulated rotation of the director $\vec{n}$ is coupled to a macroscopic mass flux velocity $\vec{v}$ and both the nematic director and the flow field remain in a single plane, the plane of the LC cell.

In Eqs. (1) and (2), $K_2$ and $K_3$ are the Frank elastic constants for twist and bend, respectively. $\gamma_1$ is the rotational viscosity coefficient, whereas $\eta_a$ and $\eta_c$ are shear

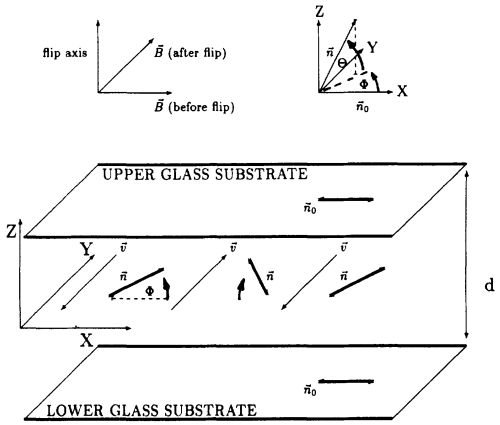


FIG. 1. Cell geometry and definition of the coordinate system.

viscosity coefficients. They are related to the more formal Leslie coefficients $\alpha_i$ of the nematic viscosity by

$$\gamma_1 = \alpha_3 - \alpha_2, \quad \eta_a = \frac{1}{2}\alpha_4 \ , \quad \eta_c = \frac{1}{2}(\alpha_4 + \alpha_5 - \alpha_2).$$

The linearized equations of motion (1) and (2) are solved by introducing the decoupled director and mass flux modes

$$n_y(x,z,t) = n_{y0}\, e^{st} \sin\left(\frac{2\pi x}{\lambda}\right) \cos\left(\frac{\pi z}{d}\right) \ , \quad (3)$$

$$v_y(x,z,t) = v_{y0}\, e^{st} \cos\left(\frac{2\pi x}{\lambda}\right) \cos\left(\frac{\pi z}{d}\right) \ , \quad (4)$$

which grow exponentially in time and obey the rigid boundary conditions. Their growth rate $s$, given by Eq. (5), is a function of the modulation wavelength $\lambda$. It is inversely proportional to an effective viscosity of the particular distortion mode under consideration,

$$s(\lambda) = \frac{\frac{\Delta\chi}{\mu_0} B^2 - K_2 \left(\frac{\pi}{d}\right)^2 - K_3 \left(\frac{2\pi}{\lambda}\right)^2}{\gamma_1 - \alpha_2^2 / \left[\eta_c + \eta_a \left(\frac{\lambda}{2d}\right)^2\right]} \ . \quad (5)$$

While the homogeneous Fréedericksz transition ($\lambda = \infty$) depends on the pure rotational viscosity $\gamma_1$, shear viscosities influence the periodic distortion modes leading to a reduction of the overall effective viscosity and thus increasing the speed of the reorientation process. However, as a result of larger director gradients, the elastic energy involved increases with decreasing wavelength. The reorientation process slows down with smaller wavelengths due to larger elastic forces. The distortion mode yielding the optimum balance between the viscous drag and elastic and magnetic forces is characterized by the maximum response speed. The relation between the wavelength $\lambda$ of the fastest growing mode which is assumed to be observed macroscopically and the external field is given by a fourth-order equation in $\lambda$:

$$\left(\frac{B}{B_c}\right)^2 = \left(\frac{1-\alpha}{\eta\alpha}\kappa\right)x^2 + \left(\frac{2\kappa}{\alpha}\right)x + \left(1+\frac{\kappa\eta}{\alpha}\right) \qquad (6)$$

$$\text{with } x = \left(\frac{2d}{\lambda}\right)^2.$$

Here $\alpha = \alpha_2^2/\gamma_1\eta_c, \eta = \eta_a/\eta_c$, and $\kappa = K_3/K_2$. $B_c = (\pi/d)\sqrt{\mu_0 K_2/\Delta\chi}$ is the critical threshold field for the homogeneous twist Fréedericksz transition. Equation (6) has finite roots for magnetic fields $B > B_s$ exceeding a second threshold field

$$B_s = \sqrt{\left(1+\frac{\kappa\eta}{\alpha}\right)}B_c.$$

For external fields $B_c < B < B_s$, the homogeneous Fréedericksz transition has maximum response speed and no structures are generated. Periodic patterns are formed at magnetic fields $B > B_s$ and their wavelengths decrease with increasing external field. The wavelength diverges for $B \to B_s$. If the periodicity of the stripe pattern is measured in dependence on the external field strength, the viscoelastic parameters $\alpha$, $\eta$, and $\kappa$ should be obtainable by fitting the data to Eq. (6). This implies that the range of validity of the linear theory is not violated in these experiments. Hence the wavelength of the pattern needs to be measured in the early stages of evolution.

In the course of the experiment, the periodicity of the structure might change due to inherent nonlinearities of nematodynamics, i.e., coupling of the individual modes. As argued by Srajer, Fraden, and Meyer [6], the observed wavelength is sligthly shifted towards larger values during the evolution of the modes.

The final state of the modulated structure is a system of periodic metastable inversion walls. They decay gradually, leaving a homogeneous twist director deformation behind. The actual processes leading to the destruction of these walls have not yet been investigated in detail.

The drawback of the deterministic linearized mode selection theory is that it is inappropriate to describe the actual evolution of the structures in time because it neglects the influence of thermal fluctuations and of nonlinearities of the system. Sagues, Arias, and San Miguel [15] developed a dynamic model which consistently includes these effects. The pattern formation is described by means of a time dependent structure factor related to the periodicity of the pattern. Whereas the wavelength of the pattern is time dependent, the value of the fastest growing mode predicted by the deterministic linearized theory is approached asymptotically in that model.

## III. EXPERIMENT

The experimental setup is given in Fig. 2. A planar cell filled with the nematic liquid crystal is placed in the pole gap of an electromagnet. The magnet provides a very homogeneous adjustable magnetic field $\vec{B}$ with a maximum induction of 800 mT. In order to study the optical transmission function of the cell, we inserted a non-magnetic

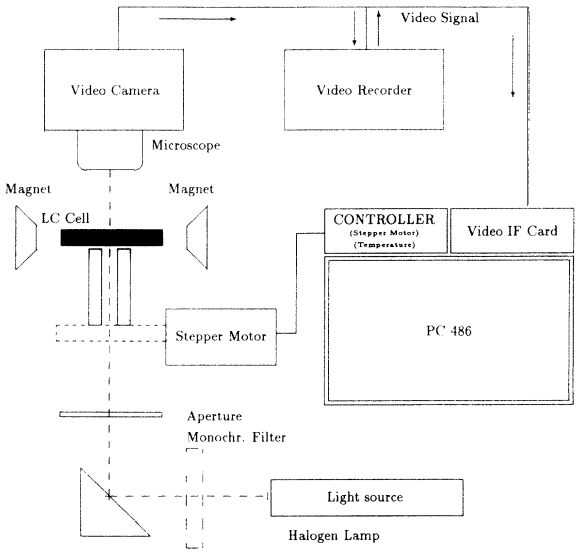


FIG. 2. Schematic view of the experimental setup. The light path is indicated by a dashed line. A halogen lamp is used as the light source. The nonmagnetic microscope is placed immediately above the sample holder in the magnetic field.

microscope between the poles of the magnet. Thus the transmission patterns of the sample cells at normal incidence could be observed directly in the magnetic field. In Fig. 2, the light path is indicated by a dashed line. A halogen lamp with monochromatic filters was used as the light source. Experiments have been performed with polarized and with nonpolarized light. The parallel light beam was directed straight through the axis of a rotatable sample holder and the transmitted light through the LC sample cell was recorded by means of a black and white video camera (370 000 pixels) mounted on top of the microscope.

Video output of the camera could be alternatively recorded by a video cassette recorder and/or further processed by a personal computer 486. Pictures were taken at a rate of 25 frames/s, which is sufficiently fast compared to the evolution of the transmission patterns.

The sample cell was mounted on top of a temperature controlled sample holder which could be rotated by a stepper motor in steps of 3.75° ($\pi/48$) around the axis of the incident light which is perpendicular to the magnetic field and normal to the cell plane. The maximum frequency of the stepper motor was approximately 100 steps/s. For most of the investigated samples this proved to be fast enough to exclude an immediate response of the director.

In the initial orientation, the surface alignment of the cell is directed parallel to the external field. The sample is then flipped by 24 steps (90°). After the flip, the optical transmission pattern is recorded. Alternatively, the cell can be placed with its surface alignment perpendicularly to the magnet at zero field and the transmission is recorded after the field is switched on. In both cases, we observed periodic transient structures.

Several nematic liquid crystals have been investi-

gated. In the experiments reported here, we used a nematic four-component mixture of *n*-alkyloxyphenyl-*m*-alkyloxybenzoates (Mischung 5 from MLU Halle):

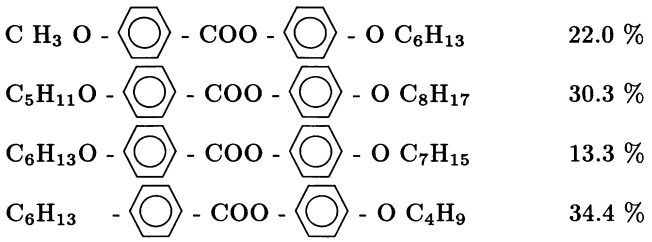


The substance is nematic at room temperature with its clearing point at 70.5 °C. Its refractive indices [16] and magnetic susceptibility [17] are well known. The elastic constants $K_1$, $K_2$, and $K_3$ and the rotational viscosity $\gamma_1$ have been determined previously by standard methods [18,19]. Their temperature dependence is given in Fig. 3. The sample cells were manufactured from $SiO_x$ oblique evaporated glass plates which provide planar surface alignment and strong surface anchoring of the director. Different cells with thicknesses between 100 and 250 $\mu$m have been prepared.

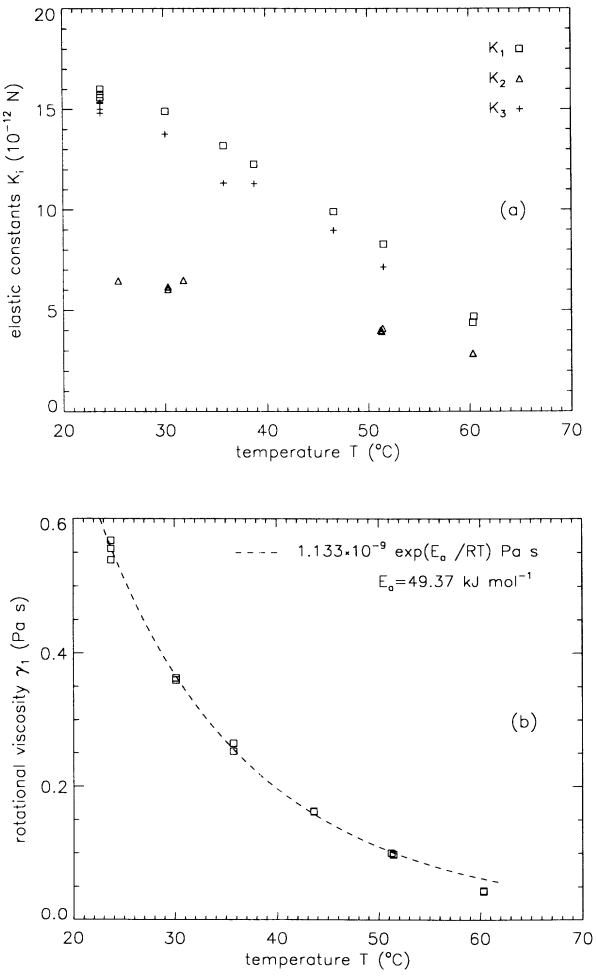


FIG. 3. Temperature dependence of (a) the elastic constants $K_1$, $K_2$, and $K_3$ and (b) the rotational viscosity $\gamma_1$ as determined from magneto-optical characteristics of a planar cell. The dashed line corresponds to an Arrhenius fit; $R$ is the molar gas constant.

## IV. RESULTS

### A. Optical transmission patterns and the evolution of twist-bend inversion walls

Figure 4 shows typical examples of the transmission patterns of LC cells with periodic structures in the twist Fréedericksz transition induced by an external magnetic field. The distance $L$ between adjacent dark stripes is related to $\lambda$ by $L = \lambda/2$. The patterns are observed without polarizers. They are also visible with crossed polarizer and analyzer inserted unless one of the polarizers is oriented normal to $\vec{n}_0$. The optical appearance changes considerably if the focal depth of the microscope is changed. The optical properties of the structures are very similar to those of Williams domains [10].

The stripes are parallel to the magnetic field, i.e., perpendicular to $\vec{n}_0$ after the $\pi/2$ flip. They appear after

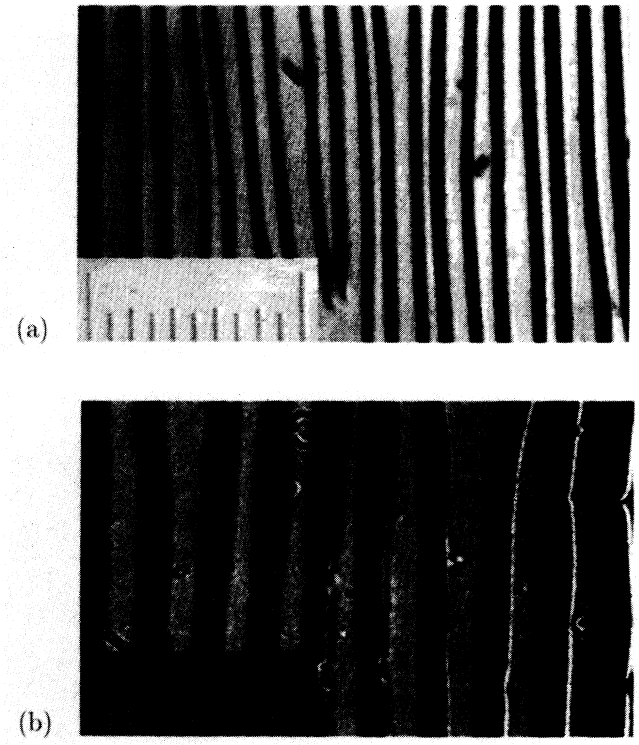


FIG. 4. Transient structures of nematic cells observed in the twist transition. The stripes are in the direction of the $\vec{B}$ field. (a) After switching a magnetic field perpendicular to $\vec{n}_0$ from 0 to 780 mT, substance PCH5 from Merck, $T = 33.3$ °C, $d = 100$ $\mu$m, white light, and crossed polarizers in the 45° orientation. (b) After a 90° flip in the magnetic field of 230 mT, substance Mischung 5, $T = 23.7$ °C, $d = 237$ $\mu$m, monochromatic light of 589 nm, and no polarizers. For comparison, ticks of a microruler which are separated by 50 $\mu$m are given in insets.

several seconds at high fields, but it may take them up to 10 min to appear at magnetic fields in the vicinity of their low field threshold. Below that threshold, no patterns are observed. A typical example of the formation of the periodic pattern is given in Fig. 5(a)–5(e).

For comparison, a time scale of the dynamics of the sample can be derived from the characteristic relaxation time of the ground mode of the cell in the homogeneous twist transition. As seen in Fig. 3, the rotational viscosity $\gamma_1 = 0.55$ Pa s at 23.7 °C is relatively large compared with other nematics (usually nematics for practical applications are optimized by the manufacturers to have a small $\gamma_1$). The relaxation time $\tau_0 = \gamma_1 d^2/(K_2\pi^2)$ is approximately 490 s for a 237 $\mu$m cell and the characteristic switching time in the homogeneous Fréedericksz transition is $\tau = \tau_0(B^2/B_c^2 - 1)^{-1}$. Inserting the $B_c$ value of the 237 $\mu$m cell (33 mT), we find a characteristic response time $\tau = 13.9$ s at a magnetic field $B$=200 mT.

The duration of the existence of the patterns is of the order of several minutes up to 3 h for the LC cells investigated. These values are strongly dependent on the cell thickness. The long lifetime of the periodic patterns suggests a formation of metastable inversion walls. The decay of the structures will be described in more detail in Sec. IV C.

The evolution of the structures is very sensitive to the flip angle. They appear at flip angles very close to 90° only. When the deviation of the flip angle from 90° is increased, the patterns become more and more irregular and finally they consist merely of isolated pairs of stripes. These stripes are still perpendicular to the direction of the initial director $\vec{n}_0$, i.e., they are no longer directed parallel to the magnetic field. Structures of decreasing amplitude have been observed at flip angles down to 85° and up to 95°, respectively. No patterns are formed if lower or higher flip angles are chosen.

Interestingly, the structures depend strongly on the flip angle but only weakly on the initial angle of the cell in the field. Provided the director field was in a stationary equilibrium state before the flip, one can evoke patterns of a comparable periodicity if the cell is flipped, for example, from an angle of −45° to +45° or from 90° back to 0. These phenomena have to be studied in more detail in the course of future experiments.

We have performed our experiments using other nematic liquid crystals too, and we found the same type of patterns in all substances investigated, including 5CB (*4-n* pentyl-*4'*-cyanobiphenyl), PCH5 (*4-n* pentylcyclohexyl-*4'*-benzonitrile), and a five component nematic mixture E2Cl (Halle), which exhibits a glassy nematic state [20].

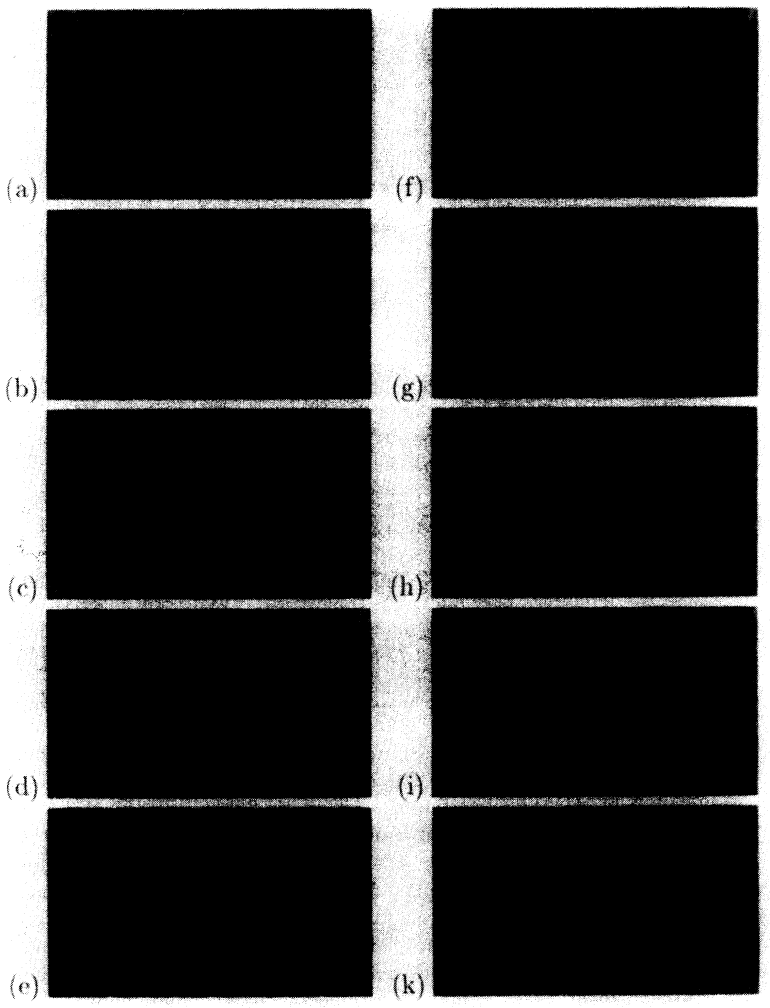


FIG. 5. Evolution of the transient pattern in the twist reorientation. Sample: Mischung 5, $T = 23.7$ °C, $d = 237$ $\mu$m, and $B$=200 mT. (a)–(e) show the evolution of the visible twist-bend walls after the 90° flip of the cell in the magnetic field and (f)–(k) show the decay of the walls during a period of more than 1 h. (a) 0 s, (b) 28 s, (c) 48 s, (d) 74 s, (e) 283 s, (f) 15 min, (g) 30 min, (h) 45 min, (i) 53 min, and (k) 72 min.

These four systems are characterized by very different viscous properties. Whereas the rotational viscosity of PCH5 is as low as 0.1119 Pa s [21] at room temperature (25 °C), it is at least one order of magnitude higher in E2Cl even at $T = 90\,^{\circ}\mathrm{C}$.

Only those experiments performed with PCH5 showed a peculiarity. The rotation speed of the stepper motor was not sufficient, and a homogeneous twist reorientation of the sample (100 $\mu$m cell) was obviously initiated during the flip; thus no stripes were observed. It was possible, however, to generate the structures, if the sample was placed in the magnet at zero field with $\vec{n}_0$ being oriented perpendicular to the pole axis and the field was subsequently switched on. Although the switching of the iron magnet takes longer than the mechanical flip, transient patterns were observed then because the symmetry of the field with respect to $\vec{n}_0$ was preserved. As seen from Fig. 4(a), the stripe distances are not very regular in this experiment, probably because the magnetic field is not constant in the course of the pattern formation process. Therefore, we have not included data from this type of experiment in the discussion of wavelengths.

By means of calculating the transmission function of our cells ($> 100$ $\mu$m) in the twisted state using the 4×4 matrix formalism, we have proved that the Mauguin limit, i.e., the condition of wave guiding, is always fulfilled [22], and that for pure twist, the director deformation is not visible in optical transmission either with or without polarizers. The polarization of the incident light follows the twist of the director along the cell normal, showing a maximum rotation in the middle of the cell. The original polarization state is reestablished after passing the complete cell. Thus, for a planar twist of the director the optical path is not influenced by the director field and the optical transmission pattern is independent of the director deformation.

The periodic patterns observed in the microscope can be explained only by assuming an additional periodically modulated tilt of the director out of the cell plane which leads to a modulation of the effective refractive index profile of the extraordinary wave which then acts as a set of cylinder lenses focusing the transmitted light. With the Mauguin limit still being valid, both the ordinary and extraordinary polarizations are still guided by the director twist, but while the ordinary wave (polarized perpendicular to the local director) remains uninfluenced, the light polarized in the local tilt plane of the director experiences a change in optical density and the optical transmission function is modulated by the lense effect mentioned above. We have verified experimentally that the optical patterns described are visible both with and without crossed polarizers, unless one of the polarizers is oriented along the polarization of the ordinary wave. Only the extraordinary wave contributes to the stripe pattern in the transmission image.

In the twist transitions found in lyotropics, similar effects have been reported [4,3]. The formation of a periodically modulated three-dimensional director deformation can be understood if free energy considerations are employed. The modulated planar twist transition predicted by the linear theory leads to the formation of metastable in-plane splay-bend inversion walls which separate regions of opposite director twist.

These walls contain large director gradients and therefore a large amount of elastic energy. Because of the anisotropy of the elastic constants of nematic LC ($K_1 \simeq K_3 > K_2$ for most rodlike low-molecular-weight nematics) these walls are unstable with respect to an out-of-plane tilt of the director when the magnetic field exceeds some critical value.

This may lead to the collapse of the walls as described in [23]. The in-plane inversion walls may, however, also convert into twist-bend walls where splay and bend deformation with high elastic energy is partially replaced by lower energy twist deformation.

A theoretical model for the description of the director field in the sample along with an energy analysis will be given in Sec. IV B.

The scenario is analogous to the formation of oblique twist-bend inversion walls in electrically driven planar cells with stripe shaped electrodes as reported currently in the literature [24]. Due to electric field inhomogeneities at the electrode edges, domains with opposite directions of director tilt appear in such cells and lead to the formation of splay-bend inversion walls. When the voltage applied at the electrodes exceeds a certain critical value these walls become unstable with respect to director perturbations which induce an additional director twist in the LC layer plane. Despite the similarity of the director deformations, the optical transmission patterns in these experiments are quite different from ours. The cell thickness is smaller by orders of magnitude in the experiments of Schmiedel ($d = 7$ $\mu$m). The effect of wave guiding is not present in such thin cells where the director deformation is in the range of the optical wavelength. Lens effects can be neglected too.

### B. Description of the director field in the inversion walls

Following the ideas outlined in [24] we have calculated the director profile within the inversion walls by a minimization procedure for the free energy. Now a single inversion wall is considered which extends from $x = -d_w/2$ to $x = d_w/2$. The free energy $W_i$ of the inversion wall per unit length of the wall is then given by

$$W_i = \int_{-d_w/2}^{+d_w/2} dx \int_{-d/2}^{+d/2} dz\; w_g(\vec{n}_i) - d_w \int_{-d/2}^{d/2} dz\; w_g(\vec{n}_e)$$

with the energy density

$$w_g(\vec{n}) = \frac{1}{2}\Big\{ K_1\,(\mathrm{div}\,\vec{n})^2 + K_2\,(\vec{n}\cdot\mathrm{rot}\,\vec{n})^2 + K_3\,(\vec{n}\times\mathrm{rot}\,\vec{n})^2 - \frac{\Delta\chi}{\mu_0}(\vec{B}\cdot\vec{n})^2 \Big\}.$$

The director field in the wall is described in terms

of director twist and tilt angles according to Fig. 1, $\vec{n} = (\cos(\theta)\cos(\phi), \cos(\theta)\sin(\phi), \sin(\theta))$. It was approximated by the separation of the variables and subsequent expansion of director twist and tilt angles into Fourier series:

$$\phi_i(x,z) = \phi_x(x)\phi_z(z) = \left[\sum_{i=0}^{N_\phi} \phi_x^{(i)} \sin\left((2i+1)\frac{\pi x}{d_w}\right)\right] \times \left[\sum_{j=0}^{M_\phi} \phi_z^{(j)} \cos\left((2j+1)\frac{\pi z}{d}\right)\right], \quad (7)$$

$$\theta_i(x,z) = \theta_x(x)\theta_z(z) = \left[\sum_{i=0}^{N_\theta} \theta_x^{(i)} \cos\left((2i+1)\frac{\pi x}{d_w}\right)\right] \times \left[\sum_{j=0}^{M_\theta} \theta_z^{(j)} \cos\left((2j+1)\frac{\pi z}{d}\right)\right]. \quad (8)$$

Outside the wall the director field is planar and depends on the $z$-coordinate only:

$$\theta_e \equiv 0\,, \quad \phi_e \equiv \pm\phi_z(z) \text{ for } x \gtrless d_w/2.$$

Since the nematic director and its derivatives have to be continuous in $x$, the Fourier coefficients are not independent of each other:

$$\phi_x^{(0)} = 1 - \sum_{i=1}^{N_\phi} (-1)^i \phi_x^{(i)},$$

$$\theta_x^{(N_\theta)} = \frac{(-1)^{N_\theta+1}}{2N_\theta+1} \sum_{i=0}^{N_\theta-1} (-1)^i (2i+1)\theta_x^{(i)}.$$

$\theta_x^{(0)}$ is a scaling factor which has been chosen $\theta_x^{(0)} \equiv 1$. Using the above assumptions the director field corresponding to the metastable inversion wall is now calculated by means of a minimization procedure for the free energy $W_i$ where the wall thickness $d_w$ and the Fourier coefficients $\theta_\alpha^{(i)}$ and $\phi_\alpha^{(i)}$ ($\alpha = x, z$) are free parameters. In a first step, the director field outside the wall, which is the static solution for the homogeneous Fréedericksz transition, is obtained if the free energy per unit area

$$W_e = \int_{-d/2}^{+d/2} dz\; w_g(\vec{n}_e)$$

is minimized by varying the coefficients $\phi_z^{(i)}$. The director field inside the wall is then calculated minimizing $W_i$ whereby $d_w$, $\phi_x^{(i)}$, $\theta_x^{(i)}$, and $\theta_z^{(i)}$ are varied. In the same way, an in-plane splay-bend inversion wall can be simulated by setting $\theta_i \equiv 0$.

For a periodic set of inversion walls with distance $L$, one has to minimize the function $W_i + LW_e$, where all parameters have to be varied simultaneously. For multiple walls, the numerical calculations of the internal structure of each wall yield results very similar to those of an isolated wall, except for a small region in the vicinity of the low field threshold $B_t$ (see Fig. 7) where the wall thickness $d_w$ is influenced by the wall distance $L$.

The results of our calculations are shown in Figs. 6 and 7. The Fourier expansion was performed choosing $N_\phi = 3, M_\phi = 5, N_\theta = 4$, and $M_\theta = 3$. This should provide a good approximation of the director field for the magnetic fields considered.

The main effect of an out-of-plane tilt of the director is the reduction of the inversion wall thickness [see Fig. 7(a)]. This means that the director field in the sample is aligned more close to the external field and thus the magnetic free energy is lowered. The director gradients in the inversion wall are, however, increased since the elastic restoring forces are smaller ($K_2 < K_1, K_3$) for the twist distortion compared to splay and bend. As can be seen from Fig. 7(b), there exists a sharp transition from the planar to the more complicated three-dimensional director distortion which is in some respect similar to the Fréedericksz transition. A threshold field $B_t \approx 2.6B_c$ is derived from our simulations. Despite the simplicity of the model used in the computations, this value is in rather good agreement with the results of the experiments.

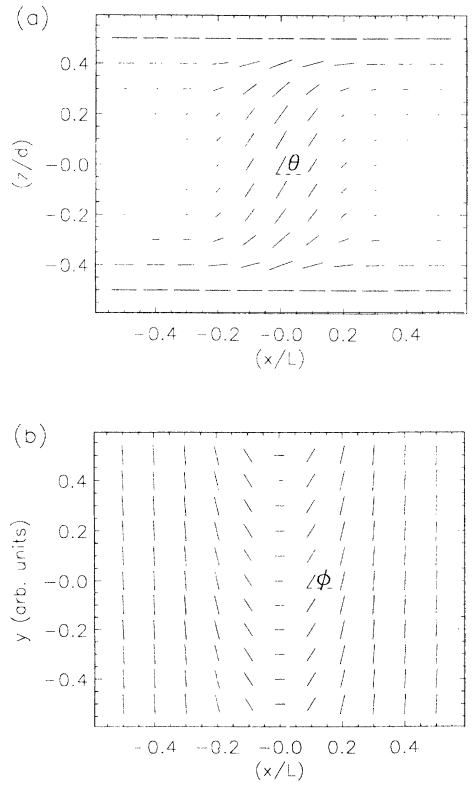


FIG. 6. (a) Schematic side view of the director field in the twist-bend inversion wall and (b) the top view onto a cross section in the cell middle plane. The angles $\theta$ and $\phi$ are indicated. $B$= 3.6 $B_c$, and $L = 0.9d$.

### C. Long time behavior and decay of the twist-bend walls

The stability of the inversion walls is particularly high at low magnetic fields. Figures 5(f)–5(k) show a typical decay of the pattern of walls. Usually, two adjacent walls extinguish each other by a pairwise annihilation. A kink is formed connecting two walls, which shifts gradually along the $y$ axis leaving a homogeneous director field behind. Two neighboring stripes often form closed loops which shrink gradually and disappear eventually. Very rarely, a single wall is observed to dissolve starting at some point without connection to a neighboring wall. The theoretical description of the very processes which lead to the extinction of the inversion walls requires a more detailed analysis of the optical patterns, including the exact calculation of their optical properties from the internal director structure.

After the flip experiments, the sample has to be converted back to its original nondeformed state before the next flip can be performed. The long relaxation times of the walls can cause problems here. In the external field, some of the walls persisted up to several hours after the flip experiment was performed. If the sample is flipped back before the inversion walls are decayed completely, one can observe even the formation of a second, superimposed structure perpendicular to the first one. The walls form closed loops then which are even more stable. The best method to bring the sample back to the undeformed state proved to be a backward flip at a magnetic field higher than $B_c$ but below $B_t$. Even then, it was necessary to wait for several minutes in order to make sure that the sample was back in its initial undeformed state, before the next experiment could be performed.

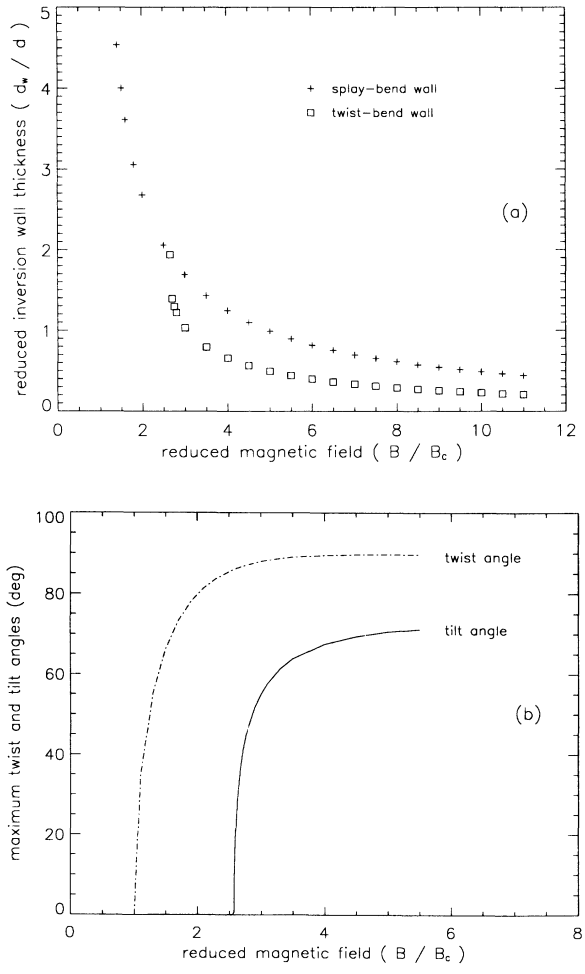


FIG. 7. (a) Wall thickness and (b) amplitudes of tilt and twist in the inversion walls, computed by free energy minimization. The maximum tilt is in the middle plane of the cell ($z$=0) in the center of the twist-bend wall, whereas the maximum twist is reached outside the wall at $z$=0. The wall thickness decreases with increasing out-of-plane tilt of the director in the walls. The critical field $B_t$, where the director field in the wall leaves the planar deformation, is clearly indicated.

### D. Fit of viscoelastic parameters

Figure 8 shows the wavelength dependence on the magnetic field. As predicted in Eq. (6), all data can be brought into good coincidence by the scaling $B/B_c$ and $\lambda/d$. The experimental data were fitted to the function $B(\lambda)$ where the parameters $\kappa$ and $B_c$ have been taken from the results for $K_2$ and $K_3$ of previous magneto-optical experiments. The quantities $\alpha$ and $\eta$ represent the fitting parameters. As the magnetic field determined by a Hall probe proved to be very stable and homogeneous, the experimental error should result mainly from the determination of $\lambda$ from the optical images. Therefore, we actually performed a least-squares fit of $\sum_i(\lambda_i^{\text{expt}}-\lambda_i^{\text{theor}})^2$. The curve is very sensitive to changes in $\alpha$, the best fit being $\alpha = 0.73 \pm 0.04$, whereas the value

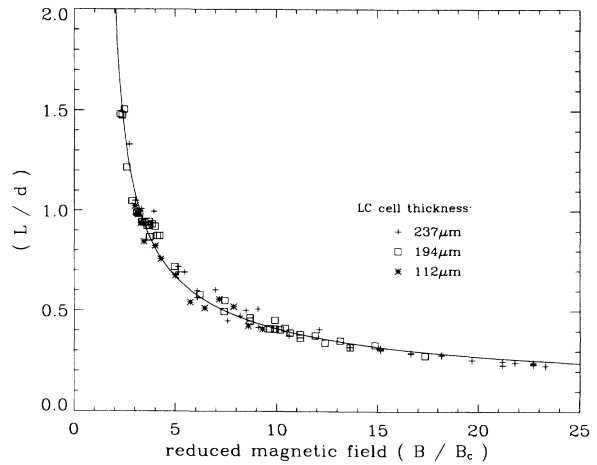


FIG. 8. Measured wavelength of the transient patterns in dependence on the magnetic field strength. $T = 23.7\,^\circ$, Mischung 5 sample. Data obtained for different cells are plotted using different symbols. They are scaled according to Eq. (6). The solid line corresponds to the best fit to Eq. (6) with the parameters $\eta = 0.5$, $\alpha = 0.73$, and $\kappa = 2.285$.

of $\eta = 0.5 \pm 0.2$ has a minor effect on the fit. The values of these parameters seem to be reasonable for typical low-molecular-weight nematics.

The critical field for the evolution of twist-bend inversion walls was determined to be $B_t = 2.2B_c$. The critical field for the evolution of periodic structures is not directly accessible in our experiment. It can be calculated using the fitting parameters to be $B_s = 1.6B_c$, where $B_c = 33$ mT for the 237 $\mu$m cell.

It was shown in Sec. II that the validity of Eq. (6) might be limited. In particular, one cannot expect the wave vector of the fastest growing mode to be independent of time. Our measurements show that the wavelengths of the structures observed are constant after the evolution of the twist-bend walls. However, it is clear that we do observe the final state of the selection process only which may differ from the results of the linearized theory outlined in Sec. II.

## V. CONCLUSIONS

We observed periodic transient patterns in the Fréedericksz transition of planar cells filled with low-molecular-weight nematics in a magnetic field. These patterns have been found in a variety of substances. They can be generated by means of a flip of the sample in the external magnetic field around an axis normal to the cell plane or alternatively by switching the field on when the cell is with its surface alignment perpendicular to the field. The structures are periodic with a wave vector parallel to the undisturbed initial director orientation $\vec{n}_0$ after the flip.

In lyotropic bulk samples it was shown that an inhomogeneous twist transition with backflow coupling dominates the homogeneous reorientation at any flip angle above 45° [25]. In contrast, the appearance of the structures reported here is very sensitive to the flip angle. They form at rotation angles in a narrow range between $\sim 85°$ and 95° only. With increasing deviation from the right angle, patterns of decreasing amplitude and finally single pairs of stripes only are observed.

The formation of the structures is not very sensitive to the initial sample orientation. If the sample was kept in any definite orientation with respect to the external magnetic field for a time sufficiently long to reach a stationary director orientation in the cell, we observed periodic patterns after the 90° flip, even though the initial director field in that case is clearly a deformed one.

The experimental data of the Mischung 5 sample at 23.7 °C can be fitted to the theoretical $\lambda(B)$ dependence given by the linearized mode selection theory. The values of the fitting coefficients are $\alpha = \alpha_2^2/(\gamma_1\eta_c)=0.73$ and $\eta = \eta_a/\eta_c=0.5$ .

In addition to the critical field $B_c$ for the homogeneous Fréedericksz transition and the critical field $B_s$ for the periodic structure formation, we have found a third critical field $B_t$ for the formation of twist-bend walls. The ratio of these fields for the given sample and temperature was $B_c : B_s : B_t = 1 : 1.6 : 2.2$.

Future investigations will be performed with thin cells where we expect to observe both the inversion walls and the initial inhomogeneous twist deformation which could not be recorded in the thick cells because of the optical wave guiding effect. This will allow conclusions on the time dependence of the periodicity of the patterns and a comparison with the deterministic linearized theory and the results of Srajer, Fraden, and Meyer [6] and Sagues, Arias, and San Miguel [15].

Recently a paper by Schwenk and Spiess [26] appeared where structures generated in the splay-bend transition of nematic side chain polymers are reported. Very similar to the results of our work, the authors observe two processes on different time scales. The first one is characterized by the formation of a planar (two-dimensional) regular director pattern. In the second, slower process the elastic energy is reduced by partial conversion of splay and bend into twist deformation by means of an out-of-plane tilt of the director.

## ACKNOWLEDGMENTS

This work was partly supported by the Deutsche Forschungsgemeinschaft (Grants Nos. Schm 902/2-1 and Sta 425/1-1). The authors are indebted to Dr. G. Pelzl and Dr. H. Kresse (Halle), who provided the refractive indices and dielectric constants of the sample, and to Ch. Cramer for optical computations.

[1] H. Haken, *Synergetics: An Introduction* (Springer-Verlag, New York, 1978).
[2] F. Lonberg, S. Fraden, A. J. Hurd, and R. E. Meyer, Phys. Rev. Lett. **52**, 1903 (1984).
[3] S. Fraden, A. J. Hurd, R. B. Meyer, M. Cahoon, and D. L. D. Caspar, J. Phys. (Paris) Colloq. **46**, C3-85 (1985).
[4] Y. W. Hui, M. R. Kuzma, M. San Miguel, and M. M. Labes, J. Chem. Phys. **83**, 288 (1985).
[5] C. R. Fincher, Jr., Macromolecules **19**, 2431 (1986).
[6] G. Srajer, S. Fraden, and R. B. Meyer, Phys. Rev. A **39**, 4828 (1989).
[7] A. J. Hurd, S. Fraden, F. Lonberg, and R. B. Meyer, J. Phys. (Paris) **46**, 905 (1985).
[8] N. Schwenk, Ph.D. thesis, Max-Planck-Institut für Polymerforschung Mainz, 1991.
[9] E. Guyon, R. Meyer, and J. Salan, Mol. Cryst. Liq. Cryst. **54**, 261 (1979).
[10] P. G. de Gennes, *The Physics of Liquid Crystals* (Clarendon Press, Oxford, 1974).
[11] L. J. Yu and A. Saupe, J. Am. Chem. Soc. **102**, 4879 (1980).
[12] J. Charvolin and Y. Hendrikx, J. Phys. (Paris) Lett. **41**, L597 (1980).

[13] E. F. Carr, Mol. Cryst. Liq. Cryst. **34**, L159 (1977).
[14] B. L. Winkler, H. Richter, I. Rehberg, W. Zimmermann, L. Kramer, and A. Buka, Phys. Rev. A **43**, 1940 (1991).
[15] F. Sagues, F. Arias, and M. San Miguel, Phys. Rev. A **37**, 3601 (1988).
[16] G. Pelzl (private communication).
[17] R. Stannarius, diploma thesis, Universität Leipzig, 1982.
[18] A. Scharkowski, Ph.D. thesis, Universität Leipzig, 1990.
[19] M. Grigutsch, diploma thesis, Universität Leipzig, 1989.
[20] R. Stannarius, W. Günther, M. Grigutsch, A. Scharkowski, W. Wedler, and D. Demus, Liq. Cryst. **9**, 285 (1991).
[21] U. Finkenzeller, T. Geelhaar, G. Weber, and L. Pohl, Liq. Cryst. **5**, 313 (1989).
[22] Ch. Cramer (private communication).
[23] A. D. Rey, Liq. Cryst. **7**, 315 (1990).
[24] H. Schmiedel, Ch. Cramer, R. Stannarius, K. Eidner, and M. Grigutsch, Liq. Cryst. **14**, 1935 (1993); Ch. Cramer, U. Kühnau, H. Schmiedel, and R. Stannarius (unpublished).
[25] P. Esnault, Ph.D. thesis, Université Joseph Fourier-Grenoble I, 1988.
[26] N. Schwenk and H. W. Spiess, J. Phys. II **3**, 867 (1993).

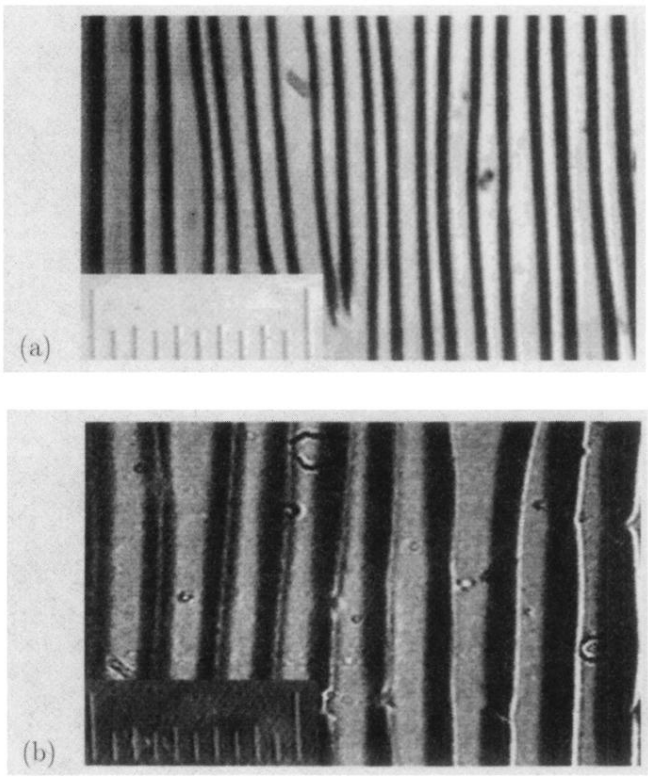


FIG. 4. Transient structures of nematic cells observed in the twist transition. The stripes are in the direction of the $\vec{B}$ field. (a) After switching a magnetic field perpendicular to $\vec{n}_0$ from 0 to 780 mT, substance PCH5 from Merck, $T = 33.3\,^{\circ}\mathrm{C}$, $d = 100\ \mu\mathrm{m}$, white light, and crossed polarizers in the 45° orientation. (b) After a 90° flip in the magnetic field of 230 mT, substance Mischung 5, $T = 23.7\,^{\circ}\mathrm{C}$, $d = 237\ \mu\mathrm{m}$, monochromatic light of 589 nm, and no polarizers. For comparison, ticks of a microruler which are separated by 50 $\mu$m are given in insets.

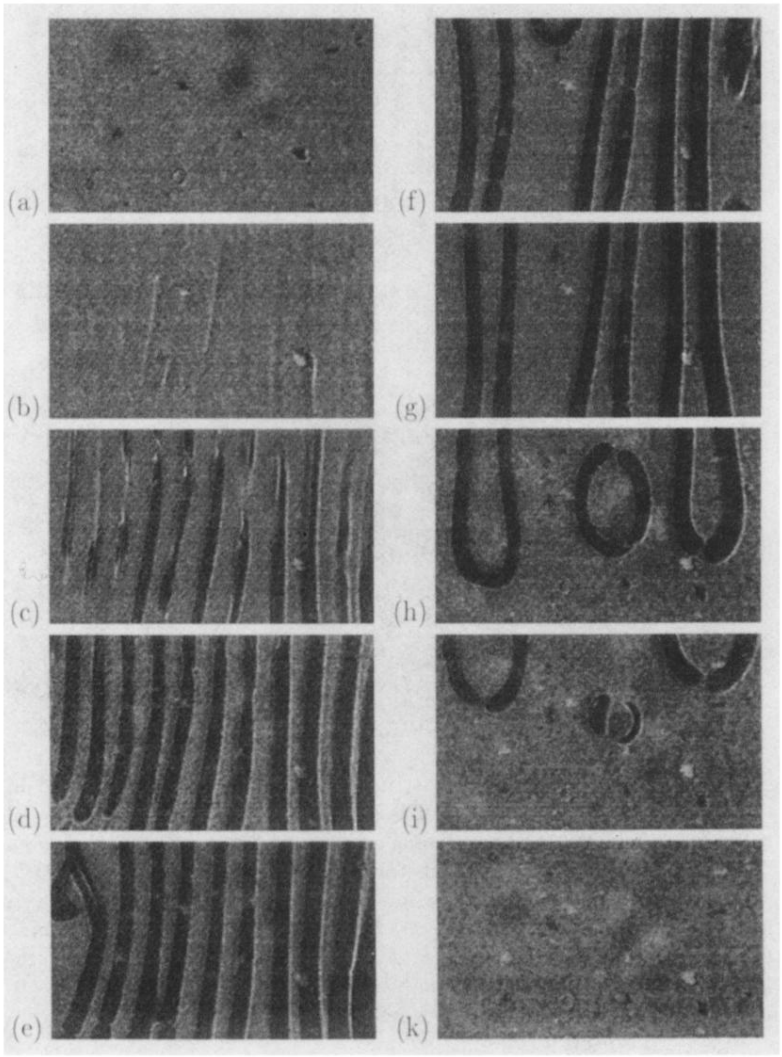


FIG. 5. Evolution of the transient pattern in the twist reorientation. Sample: Mischung 5, $T = 23.7\,^{\circ}\mathrm{C}$, $d = 237\ \mu\mathrm{m}$, and $B$=200 mT. (a)–(e) show the evolution of the visible twist-bend walls after the 90° flip of the cell in the magnetic field and (f)–(k) show the decay of the walls during a period of more than 1 h. (a) 0 s, (b) 28 s, (c) 48 s, (d) 74 s, (e) 283 s, (f) 15 min, (g) 30 min, (h) 45 min, (i) 53 min, and (k) 72 min.